View metadata, citation and similar papers at core.ac.uk

brought to you by CORE

provided by Edinburgh Research Explorer

THE UNIVERSITY of EDINBURGH

Edinburgh Research Explorer

Performance Criteria for Liquid Storage Tanks and Piping Systems Subjected to Seismic Loading

Citation for published version:
Vathi, M, Karamanos, S, Kapogiannis, IA & Spiliopoulos, KV 2017, 'Performance Criteria for Liquid Storage Tanks and Piping Systems Subjected to Seismic Loading', *Journal of pressure vessel technology-Transactions of the asme*. https://doi.org/10.1115/1.4036916

Digital Object Identifier (DOI):
10.1115/1.4036916

Link:
Link to publication record in Edinburgh Research Explorer

Document Version:
Peer reviewed version

Published In:
Journal of pressure vessel technology-Transactions of the asme

General rights
Copyright for the publications made accessible via the Edinburgh Research Explorer is retained by the author(s) and / or other copyright owners and it is a condition of accessing these publications that users recognise and abide by the legal requirements associated with these rights.

Take down policy
The University of Edinburgh has made every reasonable effort to ensure that Edinburgh Research Explorer content complies with UK legislation. If you believe that the public display of this file breaches copyright please contact openaccess@ed.ac.uk providing details, and we will remove access to the work immediately and investigate your claim.

Download date: 11. May. 2020

PERFORMANCE CRITERIA FOR LIQUID STORAGE TANKS AND PIPING SYSTEMS SUBJECTED TO SEISMIC LOADING[1]

Maria Vathi
Department of Mechanical Engineering
University of Thessaly
Volos 38334, Greece
email: mvathi@mie.uth.gr

Spyros A. Karamanos[2,3]
Department of Mechanical Engineering
University of Thessaly
Volos 38334, Greece
email: skara@mie.uth.gr

Ioannis A. Kapogiannis
Department of Civil Engineering
National Technical University of Athens
Athens 15780, Greece
email: xkapo@central.ntua.gr

Konstantinos V. Spiliopoulos
Department of Civil Engineering
National Technical University of Athens
Athens 15780, Greece
email: kvspilio@central.ntua.gr

ABSTRACT

In the present paper, performance criteria for the seismic design of industrial liquid storage tanks and piping systems are proposed, aimed at introducing those industrial components into a performance-based design framework. Considering "loss of containment" as the ultimate damage state, the proposed limit states are quantified in terms of local quantities obtained from a simple and efficient earthquake analysis. Liquid storage

[1] *An early version of the paper has been published in the proceedings of the ASME 2015 Conference on Pressure Vessels and Piping PVP2015, July 19-23, 2015, Boston, MA, USA, paper PVP2015-45700.*

[2] *Corresponding author.*

[3] *Also: School of Engineering, The University of Edinburgh, Edinburgh EH9 3FG, Scotland, UK*

tanks and the corresponding principal failure modes (elephant's foot buckling, roof damage, base plate failure, anchorage failure and nozzle damage) are examined first. Subsequently, limit states for piping systems are presented in terms of local strain at specific piping components (elbows, Tees and nozzles), against ultimate strain capacity (tensile and compressive) and low-cycle fatigue.

Modeling issues for liquid storage tanks and piping systems are also discussed, compared successfully with available experimental data, and simple and efficient analysis tools are proposed, towards reliable estimates of local strain demand. Using the above reliable numerical models, the proposed damage states are examined in two case studies: (a) a liquid storage tank and (b) a piping system, both located in areas of high seismicity.

1. INTRODUCTION

Industrial facilities (e.g. power/chemical/petrochemical plants, terminals) and their components, under seismic loading, may exhibit significant damage, which may threaten their structural integrity with severe consequences on the population, the environment and the economy. Liquid storage tanks and piping systems are considered as critical components of those industrial facilities.

The structural response of liquid storage tanks under strong seismic loading constitutes an important issue for safeguarding the structural integrity of industrial facilities, especially in refineries and power plants. Significant damages of tanks have been reported in earthquake events [1][2]. The dominant mode of tank failure is in the form of elephant's foot buckling at the tank base [3]. Other types of earthquake damages include base plate failure due to uplifting [4][5], roof damage due to excessive sloshing [6], or shell damage at nozzle areas due to non-flexible connections with piping [7]. Current practice for the seismic design of tanks is based mainly on Appendix E of API 650 standard [8]. EN 1998-4 standard [9] also contains design provisions for the seismic design of liquid storage tanks.

Furthermore, piping systems can also exhibit significant damage. Previous experimental and numerical investigations have demonstrated that most damages occur at specific locations [10][11]. Welded connections

are prone to failure, but pipe fittings (e.g. elbows, Tees) may also be areas of high stress and strain concentration, which may lead to catastrophic results [12][13]. In current design practice for piping systems, EN 13480 [14] and ASME B31.1 or B31.3 standards [15][16] are used. However, those standards contain little information on the seismic design of piping systems.

The seismic behavior of the above systems (tanks and piping) is quite complex, and significant research is necessary to understand better the mechanical behavior of critical industrial components under strong earthquake-induced cyclic loading. European research program INDUSE 2009-2012 [17] has been an important contribution towards this purpose. Combining large-scale experimental work with extensive numerical simulations, design guidelines and recommendations have been developed for the structural integrity of industrial tanks, pressure vessels and piping under strong seismic action [18][19][20][21][22][23].

Despite the above works on the mechanical behavior of tanks and pipes under strong seismic loading, the introduction of these industrial components into a performance-based design (PBD) framework, described in [24] and [25], is an open issue. Recently, a few attempts have been reported on the application of performance design concepts in the seismic design of industrial facilities [26][27][28] and to the development of seismic fragility curves [29][30][31][32]. Within this PBD framework, it is necessary to quantify all possible failure modes in terms of seismic response parameters, referred to as Engineering Demand Parameters (EDPs) and to define appropriate damage states, which classify the severity of damage [33][34]. However, up to now, these definitions have been referring mainly to building structures, whereas industrial components have not been introduced in a performance framework. It is important to realize that both liquid storage tanks and piping systems are quite different than buildings or bridges. Furthermore, tanks and piping have been considered part of mechanical equipment, designed with the "allowable stress" concept, for pressure containment. However, under severe seismic loading, they may exhibit substantial inelastic deformations, so that the existing design and analysis tools for pressure containment may not be adequate.

A national project RASOR [35] has been completed recently, on the development of numerical methodologies for assessing seismic vulnerability and risk of industrial facilities. The work of the present paper is part of the work performed within RASOR, and is aimed at introducing piping systems and liquid storage tanks (anchored and unanchored) and industrial piping in a performance-based framework. The contribution of the present paper is that it brings together all the necessary definitions and background information for industrial tanks and pipes, through appropriate quantification of the failure modes, definition of damage state levels and proposal of simple and efficient analysis tools. The proposed definitions are supported by available test data on industrial components, numerical simulation results and engineering judgment, and is being currently employed in the European research program INDUSE-2-SAFETY [36], towards developing methodologies for seismic risk assessment of critical industrial facilities.

2. PERFOMANCE CRITERIA FOR LIQUID STORAGE TANKS

The main criterion for safeguarding structural integrity of a liquid storage tank subjected to strong seismic loading is to "maintain its containment". Towards this purpose, the following failure modes, likely to occur in the course of a seismic event, should be considered.

2.1 Failure modes (limit states) for tanks

Liquid storage tanks, subjected to strong seismic loading, may exhibit one or more of the following failure modes, which are analyzed in more detail below:

- Elephant's foot buckling
- Roof damage
- Failure of base plate
- Anchor bolt failure
- Nozzle (attached piping) failure

Elephant's foot buckling

This is a major failure mode in tanks, widely encountered after severe earthquake action. It occurs when the meridional compressive stress σ_x , in conjunction with hoop tension due to internal pressure, reaches shell resistance σ_b , and results in local buckling of the tank wall at the tank bottom, in the form of bulging and folding (Figure 1). The latter can be expressed in terms of the yield stress σ_Y and an appropriate reduction factor that depends on shell slenderness [37]. Similar provisions for shell resistance against elephant's foot buckling exist in other shell design standards [8][9]. Previous investigations have shown that the occurrence of elephant's foot buckling is usually associated with tank failure; post-buckling is quite unstable, local deformations are significant and non-repairable, and shell folding at the vicinity of a nozzle may result in immediate loss of containment.

Figure 1: Elephant's foot buckling in liquid storage tanks [39].

Roof damage

In fixed roof tanks, if the maximum sloshing wave height $d_{\max}$ due to liquid free surface motion, exceeds tank freeboard δ , the tank roof may be damaged due to sloshing wave impact (Figure 2). The value of $d_{\max}$ may be computed from potential flow theory as follows [9][38]:

$$d_{\max} = 0.84 R \ddot{u}_{\max} / g \quad (1)$$

where $\ddot{u}_{\max}$ is the maximum value of convective acceleration calculated from an appropriate linear oscillator equation that describes sloshing motion [38][39] and R is the tank radius. Sloshing wave damage can be serious but not catastrophic; usually it does not result in loss of containment.

Figure 2: Tank roof damage due to sloshing [6].

Failure of base plate

This mode may occur in unanchored tanks, which exhibit base uplifting [4][5][40][41][42]. Due to uplifting, significant inelastic deformation occurs at the shell-plate welded connection, leading to either rupture because of excessive tensile strain or low-cycle fatigue damage due to repeated loading [43][44], as shown in Figure 3. More specifically,

- To identify failure due to excessive tensile strain, the maximum local tensile strain ε_T at the welded connection should be compared with the tensile resistance ε_{Tu} of the welded connection. In lieu of a detailed investigation, a value of 2% is suggested, as a conservative value for the ultimate tensile resistance ε_{Tu}, depending on the steel material and the weld defect tolerance. It is assumed that the value of yield strain $\varepsilon_Y = \sigma_Y / E$ can be used for damage initiation. In addition, the strain level of 0.5% can be used as the limit

for severe plasticization of the welded connection (ε_p). This strain is compatible with the provisions stated in the introduction of Appendix A of API 1104 standard [45].

- For a fatigue analysis of the welded connection, it is necessary to calculate the history of local strain $\varepsilon(t)$ at the weld toe induced by the seismic loading, and combine with an appropriate fatigue curve, representing the fatigue resistance of the connection. Note that strain history at the critical location is an irregular (non-constant amplitude) loading pattern, and the loading spectrum of strain action should be calculated through a "rainflow" analysis to perform a variable-amplitude fatigue analysis; the strain ranges $\Delta\varepsilon_i$ and the corresponding numbers of cycles for each strain range, n_i are calculated. To determine whether fatigue failure may occur, this spectrum should be combined with an appropriate fatigue curve, so that the number of cycles to failure N_i for each strain range $\Delta\varepsilon_i$ is obtained. Finally, using Miner's rule, a fatigue damage parameter $D = \sum_i n_i / N_i$ is calculated, where fatigue failure corresponds to a unit value [43][44].

In both failure modes, the local strain should account for geometric effects of the connection, in terms of an appropriate strain concentration factor (SNCF) [44]. The definition of the ε_{Tu} value and the choice of an appropriate low-cycle fatigue curve, together with the determination of local strain at the weld toe, may not be trivial tasks. Towards this purpose, a dedicated research effort on this subject, which combines experimental and numerical work, is planned within the INDUSE-2-SAFETY project [36].

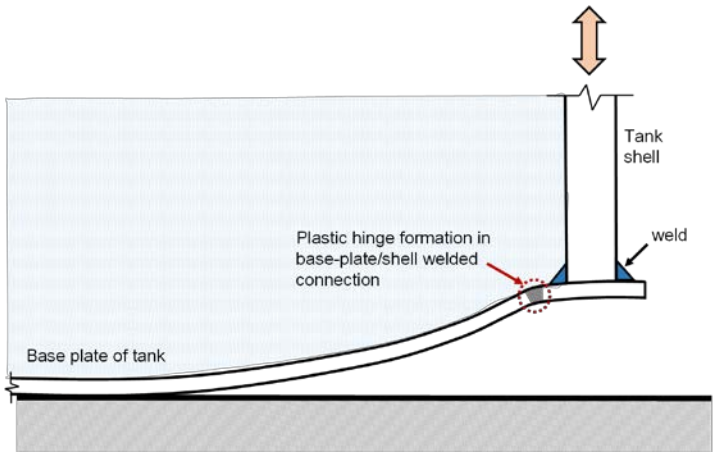

Figure 3: Schematic representation of fatigue failure of the tank-shell connection.

Anchor bolt failure

If self-anchoring is not adequate, tanks are anchored with bolts. However, the anchor system may fail because of excessive tension, as shown in Figure 4, which may occur in several forms:

- anchor bolt yielding
- anchor bolt fracture
- "prying" or shear failure of welded plates
- concrete punching shear
- anchor bolt "pull-out"

It is customary to overdesign the anchor system in terms of the last 2 modes (punching shear and pull-out), so that the failure modes of bolt or steel plate are critical. Bolt yielding or fracture may occur when the maximum tensile bolt force F induced by the seismic event exceeds a corresponding limit value:

- anchor bolt yielding:

$$F_Y = f_1 \sigma_Y A_s \tag{2}$$

- anchor bolt fracture

$$F_U = f_2 \sigma_U A_s \tag{3}$$

where σ_Y and σ_U are the yield and ultimate stress of the bolt material, A_s is the tensile stress area of the bolt, whereas f_1 and f_2 are safety factors [8][46]. The severity of anchor bolt failure may depend on the existence of rigidly connected or flexible pipe attachments. In general, anchor bolt failure may not be catastrophic and may not be associated with loss of containment. However, in the special case of rigidly connected pipes, fracture of anchor bolts may be followed by tank uplifting, resulting in fracture of the attached pipes and loss of tank containment.

In addition, failure of the steel plates of the anchor chair (Figure 4) can be identified when the maximum bolt seismic force F exceeds the prying resistance of the horizontal steel plate or the shear resistance of the

vertical plates welded to the steel tank [8]. Prying failure of the plate may not be catastrophic, but shear failure at the plate tank welded connection may result in fracture at its bottom, and immediate loss of containment. The latter failure mode can be quantified in terms of the shear stress τ developed at the welded connection compared with the yield and the ultimate shear strength of the steel material. Values of τ exceeding ultimate shear stress of the material τ_u can be considered as severe damage, associated with loss of containment due to tearing.

Figure 4: Typical anchoring in liquid storage tanks.

Nozzle (attached piping) failure

Nozzles are locations that may trigger a catastrophic failure of the liquid storage tank. The nozzle acts as an end-support for the attached pipe, and the corresponding seismic reaction forces and moments may cause significant local tank shell distortion, leading to fracture or low-cycle fatigue damage. Current design practice [8][9] adopts an empirical procedure for determining actions on nozzles, whereas flexibility of the attached piping is suggested. In general, local loads on the tank nozzle depend primarily on the seismic response of the attached piping system, rather than the response of the liquid storage tank. Therefore, this failure mode is examined in the next section, dedicated to piping systems.

Other failure modes

The above failure modes are not the only ones that may occur in a liquid storage tank under seismic loading. In several instances, buckling at the top course of the tank may also occur due to "negative pressure" because of liquid oscillations; the thin-walled shell is locally subjected to external pressure and may buckle [47][48]. Top shell buckling may be "assisted" by the impact of sloshing waves on the roof, as described above. For an attempt to model this phenomenon in a seismic design procedure, one may refer to the paper by Pappa *et al.* [47]. Furthermore, tanks with floating roofs and inflammable containment may exhibit catastrophic failure because of seal destruction and the friction of roof edge with the tank shell, which may trigger fire [49]. Modeling the behavior of a floating roof under seismic loading is out of the scope of the present study.

2.2 Damage states for liquid storage tanks

Based on the severity of damage associated with the failure modes stated in the previous paragraph, it is possible to define different damage states or levels. Four levels are considered for liquid storage tanks, shown in Table 1, motivated by the ones suggested in [30][50][51]. The levels are quantified in terms of the Engineering Demand Parameters (EDPs), which correspond to the failure modes, as shown in Table 2, and can be used for the evaluation of appropriate seismic fragility curves and risk analysis [31][32]. It is noted that level II damages require repair, whereas level I damages may not necessarily require repair. All parameters in Table 2 are defined and explained in section 2.1. In that table, the limit values of sloshing refer to API 650, par. E7.2 (Table E.7). That clause (using our notation) requires $\delta \geq d_{\max}$ for tanks essential to operate after severe earthquake, and $\delta \geq 0.7 d_{\max}$ for tanks with less stringent requirements. Inverting the above inequalities one readily obtains $d_{\max} \leq \delta$ and $d_{\max} \leq 1.4\,\delta$ respectively, which are the two limit states for no damage and minor damage used in Table 2. In addition, ε_Y is the nominal yield strain of the pipe material ($\varepsilon_Y = \sigma_Y / E$), whereas for the case of fatigue damage of the base plate, two intermediate values D_1 and D_2 should also be employed to define the range of D for level I and level II damage. The value of D_1 should correspond to damage level,

below which, damage is negligible. Values of D_1 and D_2 are proposed by the authors in the numerical example of section 5 of the present paper.

Furthermore, reliable numerical models should be employed for the computation of the EDPs. Towards this purpose, simple and efficient models for seismic analysis of liquid storage tanks and calculation of EDPs are outlined in section 4.1 of the present paper.

Level	**Description**
0	No damage
I	Minor (non-severe) damage
II	Major damage, but no loss of containment
III	Major damage with loss of containment

Table 1: Damage states for liquid storage tanks and piping systems under seismic loading.

Failure mode	Engineering Demand Parameter (EDP)	Damage State and corresponding EDP range	
elephant's foot buckling	Meridional compressive stress σ_x	$\sigma_x < \sigma_b$	0
		$\sigma_x \geq \sigma_b$	III
roof sloshing damage	Sloshing wave height $d_{\max}$	$d_{\max} < \delta$	0
		$\delta \leq d_{\max} \leq 1.4\delta$	I
		$d_{\max} > 1.4\delta$	II
anchor bolt failure	Bolt force F	$F \leq F_Y$	0
		$F_Y \leq F \leq F_U$	I
		$F > F_U$	II
bolt plate failure	Shear stress τ	$\tau \leq \tau_Y$	0
		$\tau_Y \leq \tau \leq \tau_U$	II
		$\tau > \tau_U$	III
base plate fracture	Maximum tensile local strain ε_T	$\varepsilon_T \leq \varepsilon_Y$	0
		$\varepsilon_Y < \varepsilon_T \leq \varepsilon_p$	I
		$\varepsilon_p < \varepsilon_T \leq \varepsilon_{Tu}$	II
		$\varepsilon_T \geq \varepsilon_{Tu}$	III
base plate fatigue	Damage factor $D = \sum_i \frac{n_i}{N_i}$	$D \leq D_1$	0
		$D_1 < D \leq D_2$	I
		$D_2 < D \leq 1$	II
		$D > 1$	III

Table 2: Performance criteria for liquid storage tanks under seismic loading.

3. PERFOMANCE CRITERIA FOR PIPING SYSTEMS

Prevention of "loss of containment" is the main target of seismic design of piping systems. In particular, the pipe wall should have adequate resistance against fracture and buckling, as shown in Figure 5 [52][53]. More specifically, the following failure modes may occur:

- Fracture due to excessive tensile strain
- Local buckling due to compressive action
- Low-cycle fatigue damage due to strong repeated loading

The above modes are described below.

3.1 Tensile strain limit state

In the absence of serious defects and damages, tensile capacity is controlled mainly by the strength of pipe welded connections, such as welded Tee junctions, tank and pressure vessel nozzles, pipe-to-pipe butt-welded connections or pipe-to-fitting connections (i.e. elbow, Tee, flange, reducer). To avoid fracture in those locations, the local strain induced by the seismic action should not exceed the tensile strain limit ε_{Tu}. The latter can be experimentally determined through appropriate tension tests or fracture mechanics. In lieu of such rigorous experimental or analytical methodologies, the value of the ultimate tensile strain ε_{Tu} may range between 2% and 5% [54], whereas a 3% value is proposed in EN 1998-4 [9] for steel pipelines. It is the authors' opinion that a tensile strain capacity of 2%, corresponding to welded connection rupture, is a reasonable yet conservative value that can be used for design purposes.

In pipe fittings (e.g. elbows or Tees), in addition to welds, critical areas in terms of tensile fracture may be located in the base material, away from the welds [18][19][21]. For those locations, the local strain should be computed, including geometric strain raisers, and compared with the tensile strain limit of the material. This limit can be conservatively taken equal to 2%, but larger values that may exceed 3% can be more realistic for the tensile strain limit of steel base material.

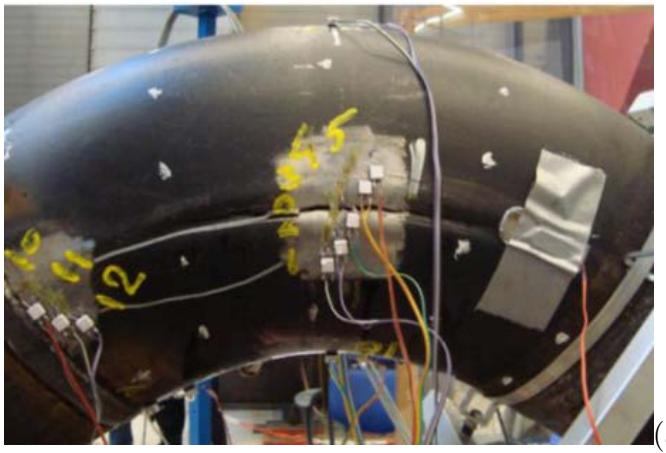
(a)

(b)

Figure 5: (a) Fracture of elbow due to low-cycle fatigue [18]; (b) local buckling of pipe elbow [52].

3.2 Compressive strain limit state

As a result of seismic action, compressive strains occur due to pipe bending. If those strains exceed a limit value (compressive strain resistance), the pipe wall buckles in the form of local wrinkles. This can be dangerous for its structural integrity; the buckled area is associated with significant strain concentrations and, in the case of repeated loading due to operational conditions, fatigue cracks may develop at the buckled area. The compressive strain resistance ε_{Cu} in the axial pipe direction depends primarily on the D/t ratio and the level of pressure; it can be estimated using the design equation (4), introduced in [55], also adopted by CSA Z662 [54]:

$$\varepsilon_{Cu} = 0.5\left(\frac{t}{D}\right) - 0.0025 + 3000\left(\frac{\sigma_h}{E}\right)^2 \qquad (4)$$

where σ_h is the hoop stress due to internal pressure, bounded by the value of $0.4\sigma_y$. Nevertheless, the onset of buckling may not be associated with immediate loss of containment, because of steel material ductility, implying a level II damage state. Beyond this limit, pipe wall folding develops at the buckled area and – in the case of bending – excessive tensile strain also occurs at the opposite side of the pipe. Thus, one has to specify a

value of ultimate compressive strain ε'_{Cu} associated with level III damage state, but no specific value is given in the literature. In the absence of relevant information, a value for ε'_{Cu} is proposed by the authors in the numerical example in section 5, based on their engineering judgement.

3.3 Low-cycle fatigue limit state

Fatigue cracks may occur under severe seismic loading in critical locations, where maximum strain occurs. In the event of a strong earthquake, piping components are subjected to repeated loading, well beyond the elastic regime of pipe material, leading to low-cycle fatigue damage at critical locations. To assess seismic-induced damage, the fatigue loading spectrum (in terms of strain range), as obtained from a "rainflow" analysis of the local strain history, should be combined with the fatigue curve of the pipe material, calculating an appropriate damage parameter. The procedure is similar to the one described for the base plate fatigue of liquid storage tanks.

In piping systems, apart from welded connections, pipe fittings (elbows or Tees) are locations of possible fatigue damage [22]. In those fittings, fatigue cracking may occur in the base material, at locations of maximum strain intensity [18][19][21].

3.4 Damage states for piping systems

The damage states associated with the seismic response of piping systems are similar to the ones presented for liquid storage tanks, shown in Table 1. These levels of damage are quantified in terms of local strain (maximum value and strain history) for the corresponding failure modes, as shown in Table 3. All parameters in Table 3 are defined and explained in sections 3.1, 3.2 and 3.3.

4. SEISMIC ANALYSIS AND MODELING VERIFICATION

An important step for conducting performance-based seismic design of liquid storage tanks and piping systems is the calculation of the corresponding Engineering Demand Parameters, using dynamic analysis models. It should be also noted that the probabilistic approach used by existing performance-based design frameworks [24][25] requires the execution of multiple nonlinear dynamic analyses, followed by verifications against all possible limit states. By consequence, the use of rigorous (detailed) models is not computationally feasible nor practical, whereas employing very simple models may not describe limit states accurately. The present section outlines modeling features for liquid storage tanks and piping systems, in an attempt to propose simple yet efficient simulation tools for the calculation of EDPs presented in the previous sections, towards reliable performance-based design of industrial components and systems.

4.1 Modeling of liquid storage tanks

The seismic behavior of liquid storage tanks is quite complex, characterized primarily by the dynamic interaction of the deformable steel tank with the moving liquid containment. Instead of detailed modeling of tank-liquid interaction considering the liquid free surface and shell-liquid interface, a simplified model can be developed that accounts for the principal response features in a simple and efficient manner [44]. The model described herein, refers to lateral (horizontal) excitation, but this approach can be modified to include rocking excitation [56] and vertical excitation [57]; the description of those models is out of the scope of the present paper.

Failure mode	Engineering Demand Parameter (EDP)	Damage state and corresponding EDP range	
tensile fracture	tensile strain ε_T	$\varepsilon_T \le \varepsilon_Y$	0
		$\varepsilon_Y < \varepsilon_T \le \varepsilon_p$	I
		$\varepsilon_p < \varepsilon_T \le \varepsilon_{Tu}$	II
		$\varepsilon_T \ge \varepsilon_{Tu}$	III
local buckling	compressive strain ε_C	$\varepsilon_C \le \varepsilon_Y$	0
		$\varepsilon_Y < \varepsilon_C \le \varepsilon_{Cu}$	I
		$\varepsilon_{Cu} < \varepsilon_C \le \varepsilon'_{Cu}$	II
		$\varepsilon_C \ge \varepsilon'_{Cu}$	III
fatigue cracking failure	damage factor $D = \sum_i \frac{n_i}{N_i}$	$D \le D_1$	0
		$D_1 < D \le D_2$	I
		$D_2 < D \le 1$	II
		$D > 1$	III

Table 3: Performance criteria for piping systems under seismic loading.

Anchored tanks

In anchored tanks, the two principal motions are taken into account, namely the "impulsive" motion, which represents the liquid and tank lateral motion due to the lateral excitation (including tank shell deformation), and the "convective" motion, associated with liquid free surface sloshing. Due to the fact that sloshing natural frequencies are substantially lower than the natural frequencies of the impulsive motion, the two motions can be considered independently [57].

The convective motion is modeled through an appropriate linear oscillator at an appropriate height (h_C), which represents the first sloshing mode (Figure 6). Consideration of additional sloshing modes is possible, introducing additional linear oscillators, but their effects on the total seismic response is not significant and

may be omitted for the purposes of the present analysis [45]. The values of sloshing frequency (ω_C), mass (m_C) and height (h_C) depend on the tank aspect ratio [38], whereas for oil and water tanks, a value of 0.5% can be considered for the damping ratio of the sloshing motion.

The impulsive motion includes the effects of tank shell deformation, and can be also expressed in terms of a linear oscillator at a certain height. The impulsive frequency (ω_i), mass (m_i) and height (h_i) depend on the aspect ratio of the tank and the tank shell thickness. The damping ratio of the impulsive motion can be taken equal to 5%. More details on the above model for deformable steel tanks under lateral seismic loading can be found in [38][57].

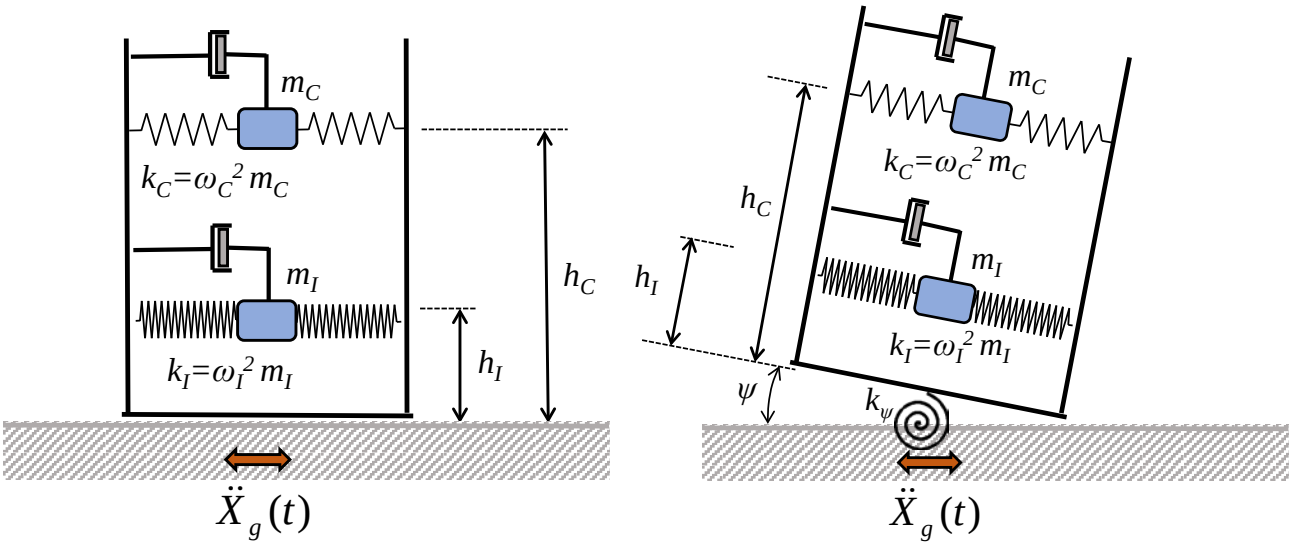

Figure 6: Simplified model for the seismic analysis of liquid storage tanks under lateral excitation $\ddot{X}_g(t)$ with no base uplifting (left) and uplifting (right) [39][41].

Unanchored tanks

The major feature of unanchored tank seismic response is base uplifting. The total motion is also decomposed in two principal motions ("impulsive" and "convective") and the basic features of the model described above for anchored liquid storage tanks are also applicable in the present case. The impulsive motion

should include tank rotation due to uplifting, using an appropriate rotational spring at the tank base that allows for base rotation ψ corresponding to uplift [42][58], as shown in Figure 6, without considering possible effects of impact between the tank base plate and the ground. The properties of the rotational spring should be determined by either using the methodology in [42], or performing a finite element analysis of the tank under lateral loading, as described in [41][44].

4.2 Modeling of piping systems and their components

The main loading parameter of piping systems under normal operating conditions is internal pressure, causing stresses and strains, mainly in the hoop cross-sectional direction. In the course of a seismic analysis procedure, pressure should be taken into account, together with pipe bending due to seismic loading, which may cause significant cross-sectional distortion (ovalization); pipe cross-section does not remain circular and this phenomenon affects substantially pipe flexibility and induces significant additional stresses and strains. These effects are more pronounced in piping components, e.g. elbows, Tee junctions and nozzles, whereas in straight parts their influence is less important [59].

Based on the above observations, it is necessary to employ numerical models, capable of describing the mechanical behavior of pressurized pipes and their piping components in the inelastic range. It has been recognized that the use of simple beam elements may not be appropriate for modeling piping systems, and the use of special-purpose beam-type elements, often referred to as "pipe elements", "tube elements" or "elbow elements" is necessary [52][60][61]. A complete presentation of the capabilities of those special-purpose elements is out of the scope of the present study. Herein, the so-called "elbow element" is employed, contained in ABAQUS/Standard element libraries [62]. It is an elaborate yet efficient element for simulating straight and curved pipe segments. It combines longitudinal beam-type deformation with cross-sectional distortion, capable of describing pressure and ovalization effects in a simple and efficient manner.

Alternatively, the use of shell elements in modeling the piping system offers a rigorous means of accounting for internal pressure and cross-sectional distortion effects, but quite expensive from the computational point-of-view. On the other hand, the use of shell elements in modeling specific piping components (such as Tees or nozzles) may be necessary, in the absence of reliable alternatives. Therefore, "elbow elements" for the straight and curved parts (elbows) of a piping system, together with shell elements for modeling Tee junctions and nozzles, constitute an efficient model, which can provide accurate predictions of the Engineering Demand Parameters (EDPs). In the following paragraphs, the validation of such a numerical model is performed, comparing the results obtained from the numerical models of the specific piping components (elbows, Tees and nozzles) with available experimental results.

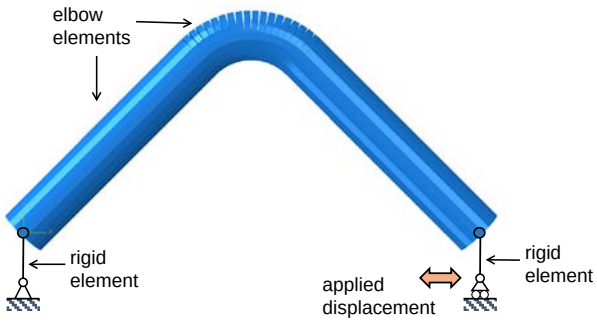

Figure 7: "Elbow-element" model for the analysis of pipe elbows.

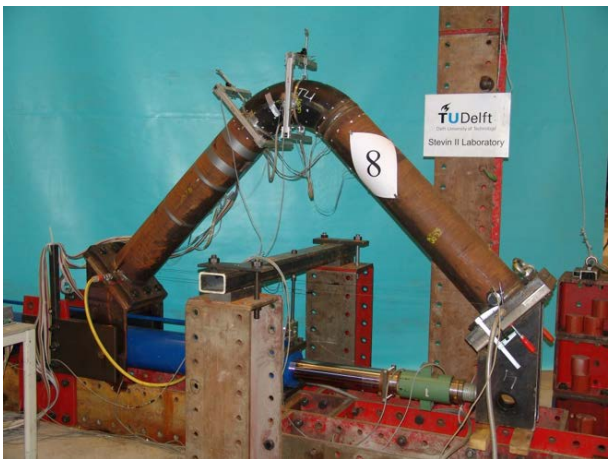

Figure 8: In-plane bending test of 8-inch-diameter pipe elbow [17][18].

Elbows

Efficient modeling of elbows, also referred to as "pipe bends", can be performed with special-purpose "elbow elements" [62]. Such a model is shown in Figure 7, which employs two-node elements, with Fourier functions in the hoop direction up to 6^{th} degree, and five elements are used for modeling a 90-degree bend. The finite element model is used to simulate an elbow bending test [17][18], shown in Figure 8. The elbow specimen is a 90-degree 8-inch SCH40 long-radius elbow subjected to in-plane cyclic bending, made of P355N material (equivalent to API 5L X52), using the loading configuration depicted in Figure 8; the 90-degree elbow is connected to two five-diameter-long straight pipes, and the entire system is subjected to two opposite displacements of alternating direction. The test has been performed at Delft University of Technology [17][18]. In Figure 9, experimental results from this test are compared with numerical predictions. The comparison shows that the numerical model is capable of describing elbow behavior quite accurately.

Tee junctions

Figure 10a shows the shell-element numerical model used for simulating a Tee junction fitting with reduced-integration four-node shell elements. This is an 8-inch-to-6-inch SCH40 Tee pipe fitting, made of P355N material. Significant effort has been made so that the size of the model is minimized to reduce the computational cost. A similar fitting has been tested experimentally under out-of-plane bending [17][21] at the University of Thessaly [17][21], as shown in Figure 10b. In Figure 11, numerical results are compared with the test data. The comparison shows a very good agreement, indicating that the numerical model can be used for simulating quite accurately the structural response of the Tee junction fitting.

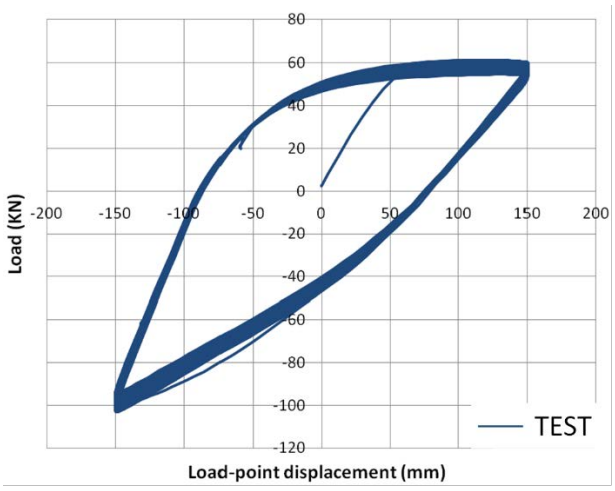

(a)

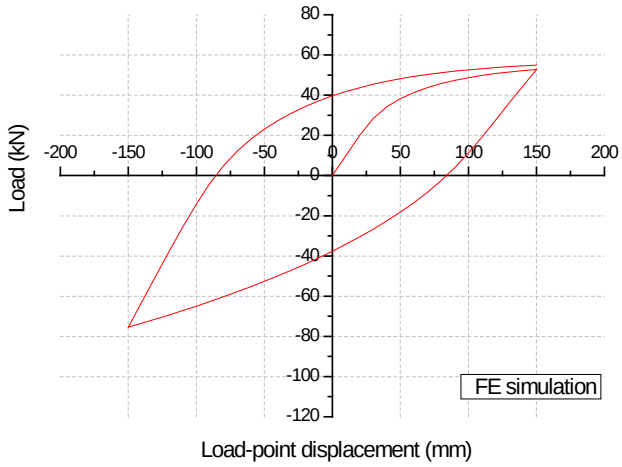

(b)

Figure 9: Comparison between (a) experimental data [17][18] and (b) numerical results (from present simplified model) for elbow in-plane bending.

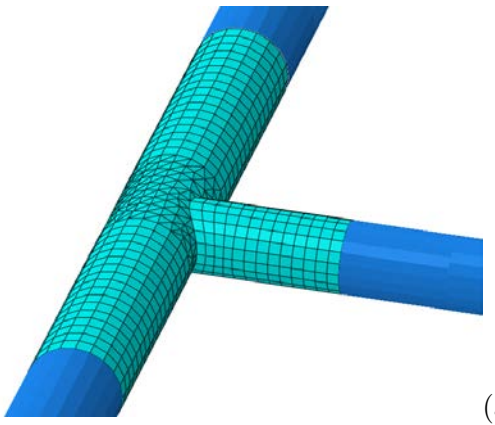

(a)

(b)

Figure 10: (a) Simplified numerical model with shell elements for the analysis of Tee junctions; (b) out-of-plane bending test of a pipe Tee junction [17][21].

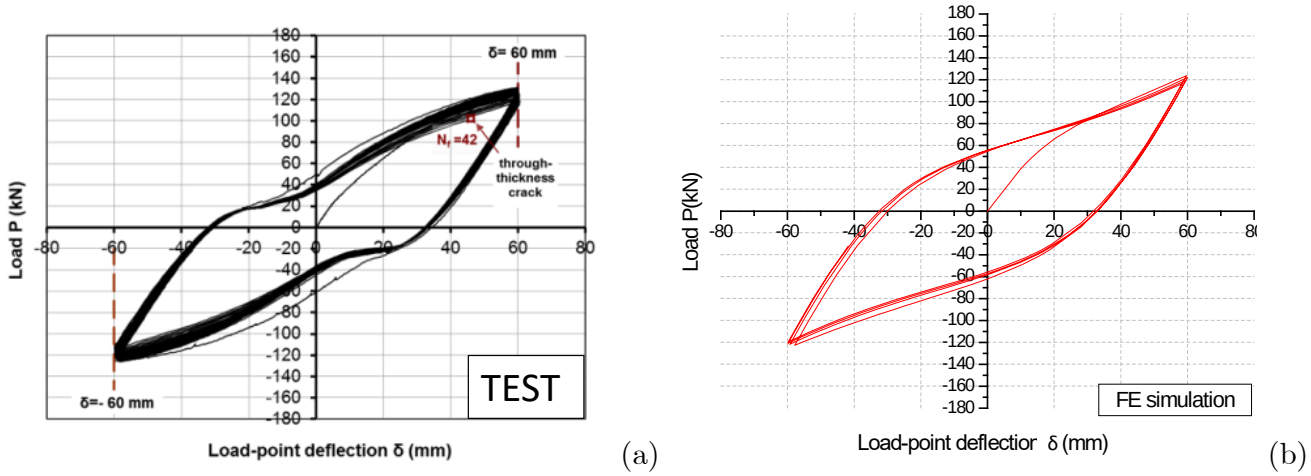

Figure 11: Comparison between (a) experimental [17][21] and (b) numerical results for Tee out-of-plane bending.

Nozzles

As noted in a previous section, pipe attachments ("nozzles"), are critical locations for the integrity of the tank-piping system. The local deformation of the tank shell in the vicinity of the connection is responsible for the development of significant stresses and strains, mainly at the weld toe locations. Under severe repeated loading, this local strain may cause fracture due to the development of fatigue cracks [17][20].

Figure 12a shows a typical finite element model for tank nozzle. The model size has been optimized to reduce the computational cost. The tank shell is 20-mm thick, butt-welded to a 30-mm-thick reinforcing plate around the nozzle, which connects to a 6-inch-diameter SCH40 pipe. Due to the large diameter of the tank, the tank shell plate is considered flat. Both materials of the pipe and the shell are P355N. The model is employed to predict the behavior of such a nozzle, denoted as P2-2, tested experimentally under lateral bending (transverse loading) conditions at Aachen University of Technology [17][20], as shown in Figure 12b. Figure 13 shows that the comparison between the experimental and the numerical results is very satisfactory.

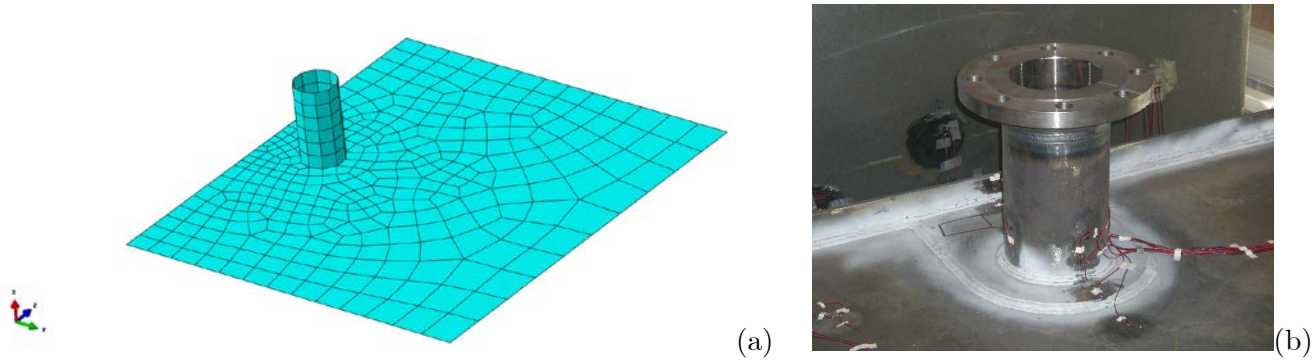

Figure 12: Simplified numerical model with shell elements for the analysis of tank nozzles. (b) Bending test of a tank nozzle [20].

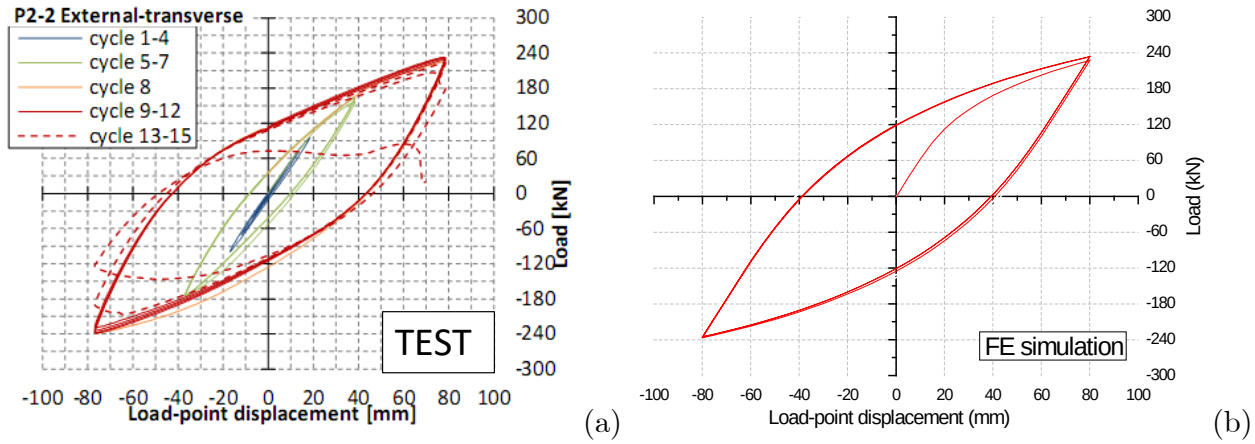

Figure 13: Comparison of (a) experimental data [17] [20], with (b) numerical results (from the present model) for nozzle loading.

5. CASE STUDIES

The above criteria are applied in two case studies; one liquid storage tank and one piping system. Both case studies are typical parts of petrochemical facilities, located in areas of significant seismicity. The present analysis is indicative, for the purpose of demonstrating the capabilities of the proposed methodology. The accelerogram of Figure 14 from the 1999 Düzce earthquake with peak ground acceleration $PGA = 0.36g$ is employed as the seismic input of the seismic analyses.

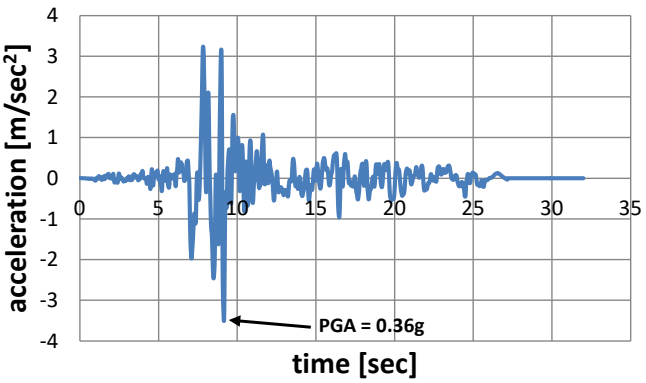

Figure 14: Seismic ground motion from Düzce earthquake 1999; peak ground acceleration (PGA) is 0.36g.

5.1 Liquid storage tank

A moderately-broad 27.8-meter-diameter tank is considered, with total height of 16.5 meters (Figure 17). The tank is modeled both as anchored and unanchored. The filling height of the tank H is equal to 15.7 (aspect ratio H/R equal to 1.131). The tank thickness varies from 6.4 mm at its top course to 17.7 mm at its bottom course and the bottom plate is 6 mm thick with an 8-mm-thick annular plate. The contained liquid is water ($\rho = 1000$ kg/m^3) and the material of the tank shell, the bottom plate and the roof is structural steel S235 (equivalent to A36 steel) with yield stress $\sigma_y = 235$ MPa.

In the anchored case, M42 class 10.9 anchor bolts are considered, with yield and ultimate tensile strength, σ_{Yb} and σ_{Ub}, equal to 900 and 1000 MPa respectively. The effective tensile stress area of the anchor bolt A_s is equal to 1120 mm^2 and bolt spacing around the tank is equal to 1.8 m. The Strain Concentration Factor (SNCF) value for this tank has been calculated equal to 3, based on the application of Stowell-Hardrath-Ohman equation for inelastic notch strain [63], and the cyclic stress-strain curve of the steel material. Furthermore, a linear $\log \Delta\varepsilon$ - $\log N$ fatigue curve is used:

$$\Delta\varepsilon = 0.05 N^{-0.33} \qquad (5)$$

which follows the mean curve of BS 7608 [64], expressed in terms of strain range.

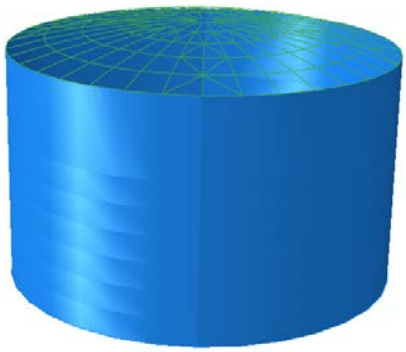

Figure 15: Liquid storage tank with aspect ratio H/R=1.131.

The seismic response of the tank is obtained using the simplified models shown in Figure 6. For the case of unanchored tanks, a finite element analysis under lateral loading is performed first, as described in [44], so that the rotational spring due to uplifting mechanism is determined. It is noted that for a comprehensive performance assessment, a suite of 20-30 ground motion records is typically employed at several intensity levels to capture the entire range of structural performance [33]. Herein, for illustrative purposes, only a single ground motion is employed in the form of the Düzce earthquake record in Figure 15, where its ground acceleration values are multiplied by a factor λ, to obtain an accelerogram with the desired PGA value. At each PGA value, a time history analysis is conducted, and the tank is verified against all failure modes under consideration. The assessment process described in detail below, simply needs to be repeated for additional accelerograms.

Figure 16 and Figure 17 show typical responses of the liquid storage tank in terms of the overturning moment and the local strain at the base plate-tank connection. Tank performance is presented in Table 4, Table 5, Table 6, Table 7 and Table 8 in terms of different performance criteria for the failure modes under consideration. The results show that roof damage due to sloshing can be possible only for strong seismic action. In the anchored case, elephant's foot buckling (Table 4) or bolt failure (Table 6) may occur for PGA equal to 0.50g. The present analysis for the unanchored case does not account for possible impact between the tank and

the ground, which may affect the axial stress developed at the tank shell bottom. In the unanchored case, the results indicate that severe damage of base plate connection may occur (damage state III) due to excessive local strain (Table 7). For the purposes of performing a fatigue design of the base plate, the values of D_1 and D_2 in Table 2 are taken 0.50 and 0.80 respectively, based on engineering judgement. A special-purpose investigation on this subject is being currently performed in the course of the INDUSE-2-SAFETY project [36], involving both experimental and numerical work, towards assessing and improving the above analysis methodology, mainly with respect to the values of the EDPs related with the limit state definitions.

PGA [g]	anchor	Engineering Demand Parameter		Damage state
		Action σ_x [MPa]	Resistance σ_b [MPa]	
0.25	yes	16.53	30.7	0
	no	8.26		0
0.36	yes	23.61		0
	no	11.04		0
0.50	yes	32.06		III
	no	15.89		0

Table 4: Response of tank in terms of elephant's foot buckling for several PGA levels.

PGA [g]	anchor	Engineering Demand Parameter		Damage State
		Action $d_{\max}\ [m]$	Resistance (i) $\delta\ [m]$ (ii) $1.4\delta\ [m]$	
0.25	yes	0.85	(i) 0.814 (ii) 1.14	I
	no	0.59		0
0.36	yes	1.22		II
	no	1.22		II
0.50	yes	1.70		II
	no	2.40		II

Table 5: Response of tank in terms of roof sloshing damage for several PGA levels.

PGA [g]	anchor	Engineering Demand Parameter		Damage State
		Action $F\ [kN]$	Resistance (i) $F_Y\ [kN]$ (ii) $F_U\ [kN]$	
0.25	yes	510.5	(i) 806.4 (ii) 1008	0
0.36		729.3		0
0.50		1021.0		II

Table 6: Response of tank in terms of anchor bolt failure for several PGA levels.

PGA [g]	anchor	Engineering Demand Parameter		Damage State
		Action ε_T	Resistance (i) ε_Y (ii) ε_p (iii) ε_{Tu}	
0.25	no	0.011 (L)	(i) 0.0011 (ii) 0.005 (iii) 0.02	II
		0.016 (R)		II
0.36		0.018 (L)		II
		0.022 (R)		III
0.50		0.028 (L)		III
		0.029 (R)		III

Table 7: Response of tank in terms of base plate fracture for different PGA levels, at the left (L) and right (R) side of the tank.

PGA [g]	anchor	Engineering Demand Parameter		Damage State
		Action D	Resistance (i) D_1 (ii) D_2	
0.25	no	0.045 (L)	(i) 0.5 (ii) 0.8 (iii) 1	0
		0.099 (R)		0
0.36		0.140 (L)		0
		0.158 (R)		0
0.50		0.347 (L)		0
		0.232 (R)		0

Table 8: Response of tank in terms of base plate fatigue for several PGA levels, left (L) and right (R) sides.

5.2 Piping system

Figure 18a shows the piping system under consideration. It comprises two main lines, an 8-inch-diameter line and a 6-inch-diameter line connecting in a Tee junction. Both pipes are SCH40, pipe material is P355N and the pipes are pressurized with 4 MPa. There exist 4 elbows, three in the 8-inch pipe and one in the 6-inch

pipe. The 6-inch pipe is connected to a liquid storage tank; at the nozzle level, the tank thickness is equal to 20 mm, but it is increased locally to 30 mm. Regarding the supports, the pipes are considered pinned in specific joints (Figure 18b), while the rest of the supports restrain only the vertical movement. The end nodes of the pipe are considered as rollers and two pinned supports are located at the end of two elbows. Finally, a part of the 8-inch pipe is elevated and supported by a steel pipe rack, fixed at its base. The pipe rack consists of steel S275 and steel sections HEB200, IPE200 and L120×10 for columns, beams and bracings respectively. The dimensions of the structure are 8.5m along the z-axis and 2.5m along the x-axis. The pipe rack has two floor levels, 2m and 4m above the ground. During the design of the pipe rack, extra loads and masses were taken into account, each floor carries 8 pipes full with water. The connection between the pipe and the pipe rack is such that their relative movement is prevented. The load and the mass of the liquid were also taken into account. In addition, loads and masses have been added at both levels of the pipe rack, in order to account for the presence of more pipes.

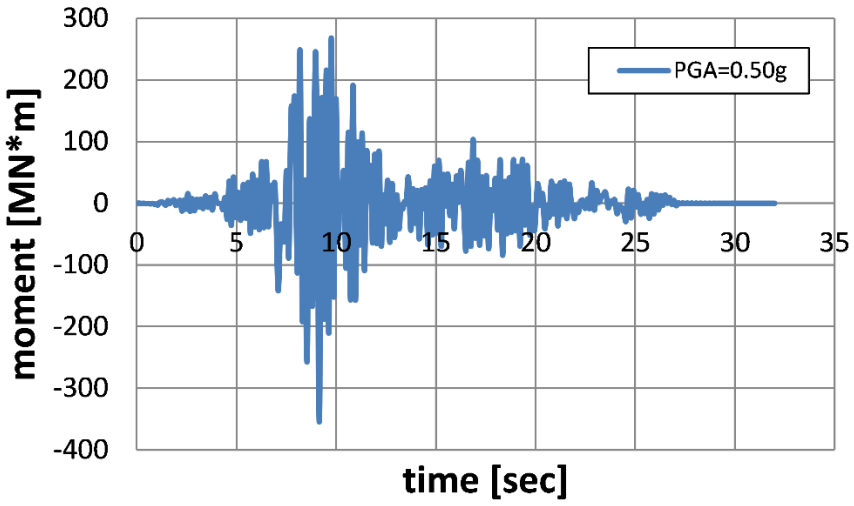

Figure 16: Time-history of the overturning moment for the anchored tank, for PGA equal to 0.50g.

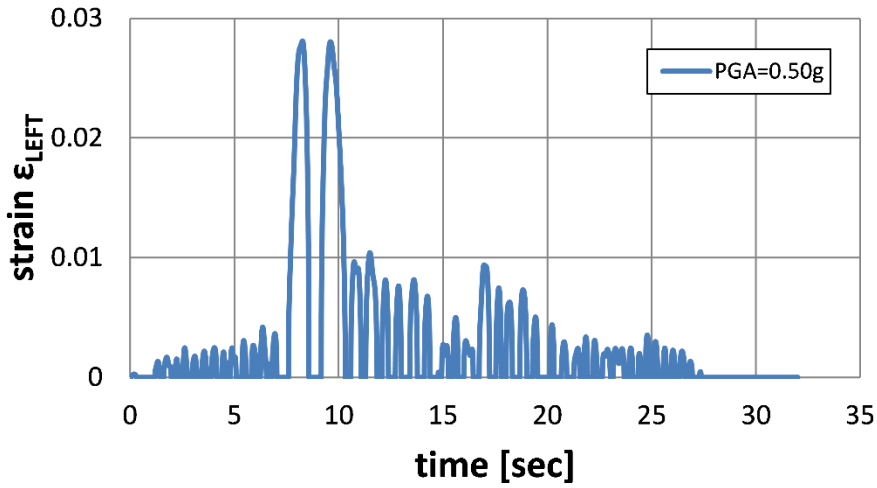

Figure 17: Time-history of bending strains at the plate-shell connection at the "left" side of the tank for PGA equal to 0.50g.

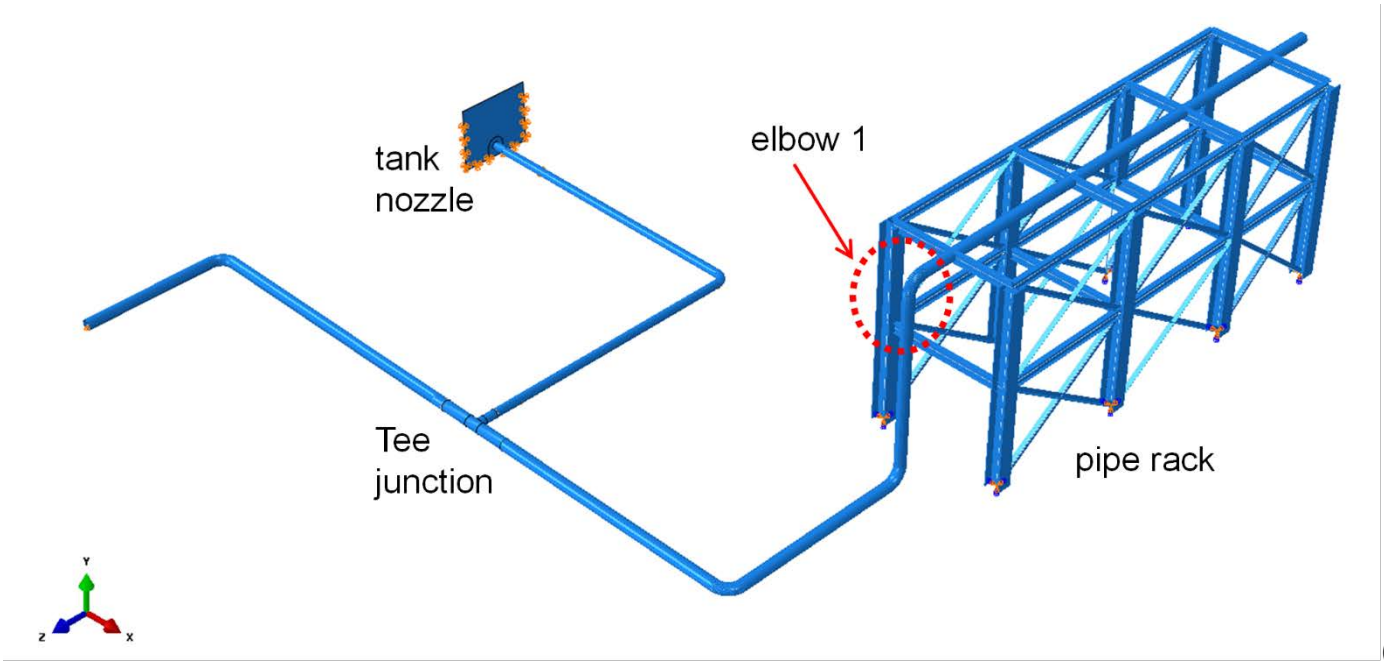

(a)

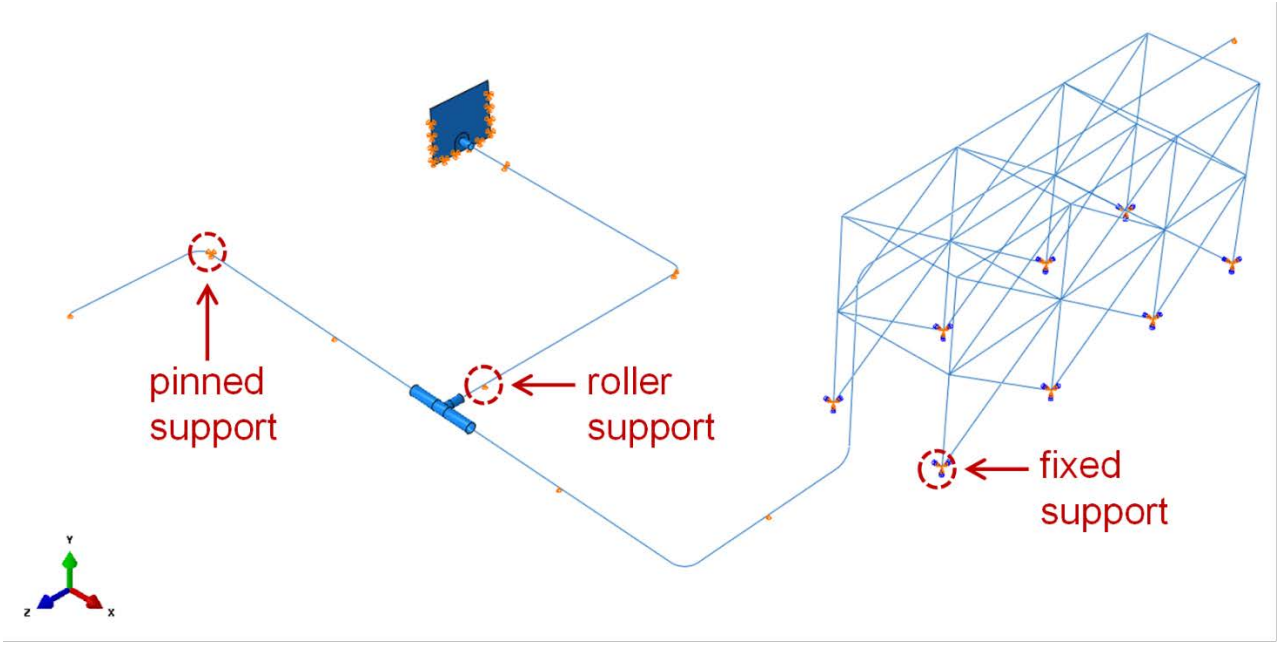

(b)

Figure 18: General layout of piping system under consideration; (a) components of the piping system; (b) support locations of the piping system.

The current model contains all critical parts of the piping system and considers the dynamic amplification of the pipe-rack and the dynamic interaction of the pipe with the pipe rack in a rigorous manner. The interaction between the pipe and the tank is also considered through the local flexibility of the nozzle model.

The piping system is subjected to seismic motion at its supports, in the form of Düzce earthquake (Figure 14), considering two levels of peak ground acceleration; 0.36g (no amplification of the seismic input) and 0.50g (considering an amplification factor equal to 1.4). In both cases, the critical component is the upper elbow near the pipe rack, denoted as "elbow 1" in Figure 18a. The response of this elbow at flank location is reported in Figure 19 and in Figure 20 in terms of local strain.

The results of the above analysis indicate the development of significant strains induced by the seismic loading, well into the inelastic region, but they are less than the strains corresponding to level III damage. In particular, considering the case of PGA equal to 0.50g,

- the maximum tensile strain is 1.35%, considerably greater than the plastic limit strains ($\varepsilon_P = 0.5\%$), but less than the tensile strain limit of 2%. Therefore, it corresponds to a damage state II, according to Table 3.
- the maximum compressive strain on the elbow is equal to 0.86% which is below the critical compressive strain ε_{Cu}, which is equal to 1.66%, thus corresponding to damage state I, according to Table 3.
- performing a fatigue analysis of the elbow, the damage factor D, for PGA equal to 0.50g, is equal to 0.5%. This value is very low, corresponding to damage state 0. This implies that the seismic motion under consideration induces a rather insignificant amount of fatigue damage at this pipe component and for the piping system under consideration.

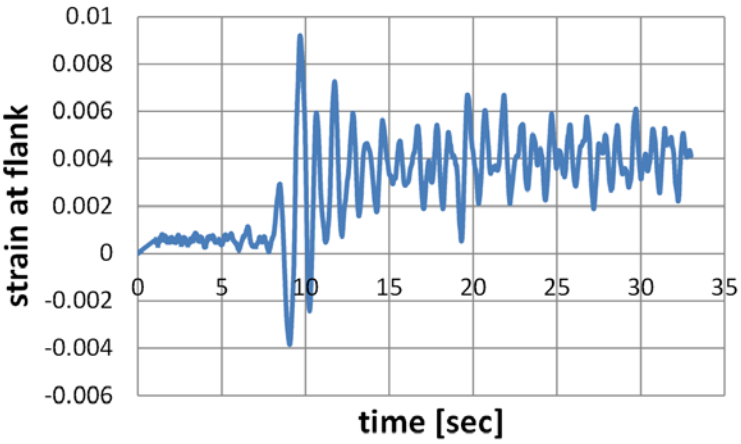

Figure 19: Response of the critical elbow of the piping system to Düzce earthquake (PGA=0.36g).

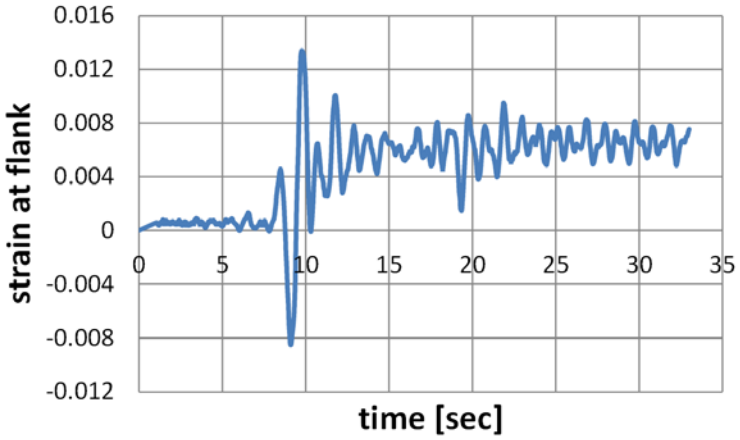

Figure 20: Response of the critical elbow of the piping system to amplified Düzce earthquake (PGA=0.50g).

6. CONCLUSIONS

This paper describes the definition of damage states for introducing liquid storage tanks and piping systems in a performance-based seismic design framework. For both systems, the main failure modes have been identified and quantified in terms of appropriate Engineering Demand Parameters (EDPs), and simple yet efficient dynamic analysis tools have been proposed. More specifically, the following issues have been addressed in the present paper:

1. Four damage states (levels) have been defined, from level 0 (no damage) to level III (severe damage and loss of containment).
2. Failure modes (limit states) for liquid storage tanks and piping systems have been identified and expressed in terms of appropriate Engineering Demand Parameters (EDPs).
3. Numerical models for tanks and piping systems have been proposed, for the simple and efficient calculation of EDP values under seismic loading, in the course of performance-based seismic design and assessment.
4. Each mode of failure has been associated with a specific limit state, quantified through an appropriate level of EDP values, based on available experimental testing, numerical computations, and engineering judgement.

The above are applied in two typical case studies (tank and piping system) from existing industrial plants. The proposed damage state definitions and numerical tools can be used for developing reliable vulnerability and risk assessment methodologies, towards increasing the safety of industrial facilities against severe seismic loading.

ACKNOWLEDGMENTS

This research has been co-financed by the European Union (European Social Fund – ESF) and Greek national funds through the Operational Program "Education and Lifelong Learning" of the National Strategic Reference Framework (NSRF) - Research Funding Program: THALES, Investing in knowledge society through the European Social Fund. The two last authors wish to acknowledge the financial support by the State Scholarships Foundation (IKY), through program “Research Projects for Excellence IKY/SIEMENS. Finally,

the authors would like to thank in particular Dr. Dimitrios Vamvatsikos, Assistant Professor at NTU Athens, for his continuous and valuable support on this subject, throughout the RASOR research project.

REFERENCES

[1] Haroun, M. A. (1983). "Behavior of unanchored oil storage tanks: Imperial Valley, earthquake", *J. Tech. Topics in Civil Engineering.,* ASCE, vol. 109, No. 1, pp. 23-40.

[2] Manos, G. C., and Clough, R. W. (1985). "Tank damage during the May 1983 Coalinga earthquake", *Earthquake Engineering and Structural Dynamics,* Vol. 13, No. 4, pp. 449-466.

[3] Manos, G. C. (1986). "Earthquake tank-wall stability of unanchored tanks", *Journal of Structural Engineering*, ASCE, Vol. 112, pp. 1863-1880.

[4] Peek, R. (1988). "Analysis of unanchored liquid storage tanks under lateral loads", *Earthquake Engineering and Structural Dynamics*, Vol 16, No. 7, pp. 1087-1100

[5] Natsiavas, S., Babcock, C.D. (1988). "Behavior of unanchored fluid-filled tanks subjected to ground excitation", *Journal of Applied Mechanics*, ASME, Vol. 55, No. 3, pp. 654-659.

[6] American Society of Civil Engineers (2000). *Izmit (Kocaeli) Turkey, earthquake of August 17, 1999*, A. K. Teng (editor), Technical Council on Lifeline Earthquake Engineering, Reston, VA.

[7] Vasilescu, S. and Ilinca, C. (2014). "A strength calculation of a nozzle using comparative methods", *Key Engineering Materials*, Vol. 601, pp. 84-87.

[8] American Petroleum Institute (2007). *Seismic Design of Storage Tanks - Appendix E, Welded Steel Tanks for Oil Storage*, API 650, 11th Edition, Washington, D. C.

[9] European Committee for Standardization (2006). *Silos, tanks and pipelines, Eurocode 8, part 4*, CEN/TC 250, EN 1998-4, Brussels.

[10] Ravi Kiran, A., Agrawal, M. K., Reddy, G. R., Singh, R. K., Vaze, K. K., Ghosh, A. K. and Kushwaha, H. S. (2007). "Fatigue-Ratcheting Study of Pressurized Piping System under Seismic Load", *SMiRT 19 Conference*, Toronto, Canada.

[11] Tsunoi, S. and Mikami, A. (2007). "Comparison of failure modes of piping systems with wall thinning subjected to in-plane, out-of-plane and mixed mode bending under seismic load - computational approach", *ASME PVP 2007 Conference*, San Antonio, Texas.

[12] Sakai M., Saito, K. and Hagiwara, Y. (1997). "Fatigue damage evolution of thin-walled short elbow under seismic loading", *SMiRT 14 Conference*, Lyon, France.

[13] Yahiaoui, K., Moffat, D. G., Moreton, D. N. (1995). "Cumulative damage assessment of pressurised piping branch junctions under in-plane run pipe simulated seismic bending", *International Journal of Pressure Vessels and Piping*, Vol. 63, No. 2, pp. 119-128.

[14] European Committee for Standardization (2011). "Metallic Industrial Piping – Part 3: Design and Calculation", EN 13480-3, CEN, Brussels.

[15] American Society of Mechanical Engineers (2012). *Power Piping*, ASME B31.1 standard, Washington DC.

[16] American Society of Mechanical Engineers (2012). *Process Piping*, ASME B31.3 standard, Washington DC.

[17] Pappa, P. *et al.* (2012). "Structural safety of industrial steel tanks, pressure vessels and piping systems under seismic loading (INDUSE)," *RFCS Project Final Report*, Brussels, http://bookshop.europa.eu/.

[18] Varelis, G. E., Karamanos, S. A., and Gresnigt, A. M. (2013). "Steel Elbow Response Under Strong Cyclic Loading.", *Journal of Pressure Vessel Technology*, ASME, Vol. 135, No.1, Article Number: 011207.

[19] Varelis, G. E., Ferino J., Karamanos, S. A., Lucci A., Demofonti G., (2013). "Experimental and Numerical Investigation of Pressurized Pipe Elbows under Strong Cyclic Loading Conditions", *ASME 2013 Pressure Vessels & Piping Division Conference,* PVP2013-97977, Paris, France.

[20] Wieschollek M., Hoffmeister B., and Feldmann M. (2013). "Experimental and Numerical Investigation on Nozzle Reinforcements", *ASME 2013 Pressure Vessels & Piping Division Conference,* PVP2013-97430, Paris, France.

[21] Papatheocharis, T., Diamanti, K., Varelis, G. E., Perdikaris, P. C. and Karamanos, S. A., (2013). "Experimental and numerical investigation of pipe Tee junctions under strong cyclic loading", *ASME 2013 Pressure Vessels & Piping Division Conference,* PVP2013-97626, Paris, France.

[22] Ferino, J., Lucci, A., Demofonti, G. (2013). "Pressurized Flanged Joints Subjected to Bending Cyclic Loading – Finite Element Analyses", *ASME 2013 Pressure Vessels & Piping Division Conference,* PVP2013-97894, Paris, France.

[23] Reza, S., Bursi, O. S., Abbiati, G., Bonelli, A. (2013). "Pseudo-dynamic heterogeneous testing with dynamic substructuring of a piping system under earthquake loading", *ASME 2013 Pressure Vessels & Piping Division Conference,* PVP2013-97441, Paris, France.

[24] Yang, T. Y., Moehle, J., Stojadinovic, B. and Der Kiureghian A. (2009). "Seismic Performance Evaluation of Facilities: Methodology and Implementation,", *Journal of Structural Engineering*, Vol. 135, No. 10, pp. 1146-1154.

[25] Krawinkler H., Zareian F., Medina R. A., and Ibarra L. F. (2006). "Decision support for conceptual performance-based design.", *Earthquake Engineering and Structural Dynamics*, Vol. 35, No. 1, pp.115–133.

[26] Ju, S., and Jung, W. Y. (2013). "Evaluation of Performance Requirements for Seismic Design of Piping System", *International Journal of Civil, Environmental, Structural, Construction and Architectural Engineering*, Vol. 7, No. 2.

[27] Bursi, O. S., Reza, M.S., Abbiati, G., Paolacci, F. (2015). "Performance-based earthquake evaluation of a full-scale petrochemical piping system", *Journal of Loss Prevention in the Process Industries*, Vol. 33, pp. 10-22.

[28] Bursi, O. S., Paolacci, F., Reza, M. S., Alessandri, S., Todini, N. (2016). "Seismic Assessment of Petrochemical Piping Systems Using a Performance-Based Approach", *Journal of Pressure Vessel Technology*, ASME, Vol. 138, No. 3, Article Number: 031801.

[29] Koike, T., Imai, T., and Ogikubo, T. (2008). "Performance-Based Design of Steel Tanks Under Seismic Risks.", *14TH World Conference on Earthquake Engineering*, Beijing, China.

[30] O' Rourke, M. J., Eeri, M., and So, P. (2000). "Seismic Fragility Curves for On-grade Steel Tanks," *Earthquake Spectra*, Vol. 16, New York, USA.

[31] Fabbrocino, G., Iervolino, I., Orlando, F., Salzano, E. (2005). "Quantitative Risk Analysis of Oil Storage Facilities in Seismic Areas," *Journal of Hazardous Materials*, Vol. 123, pp. 61-69.

[32] Salzano, E., Iervolino, I., Fabbrocino, G. (2003). "Seismic Risk of Atmospheric Storage Tanks in the Framework of Quantitative Risk Analysis," *Journal of Loss Prevention in the Process Industry*, Vol. 16, pp. 403-409.

[33] Fragiadakis M., Vamvatsikos D., Lagaros N., Karlaftis M., and Papadrakakis M. (2015). "Seismic Assessment of Structures and Lifelines.", *Journal of Sound and Vibration*, Vol. 334, pp. 29-56.

[34] Vamvatsikos D., Kazantzi A., and Aschheim M.A. (2016). "Performance-based seismic design: Avant-garde and code-compatible approaches.", *ASCE-ASME Journal of Risk and Uncertainty in Engineering Systems, Part A: Civil Engineering*, Vol. 2, No. 2, Paper No. C4015008.

[35] Papadopoulos, V. *et al.* (2015). "Risk assessment for the seismic protection of industrial facilities", *Final Report, RASOR project,* THALES: http://excellence.minedu.gov.gr/thales/en/thalesprojects/379422

[36] Bursi, O. S., *et al.* (2015). "Component Fragility Evaluation, Seismic Safety Assessment and Design of Petrochemical Plants Under Design-Basis and Beyond-Design-Basis Accident Conditions," Mid-Term Report, INDUSE-2-SAFETY project 2014-2017, *RFCS program, European Commission*, Brussels, Belgium, website: http://www.induse2safety.unitn.it/.

[37] European Committee for Standardization (2007). *Strength and Stability of Shell Structures, Eurocode 3, Part 1-6*, CEN/TC 250, EN 1993-1-6, Brussels.

[38] Ibrahim, R. (2005). *Liquid Sloshing Dynamics: Theory and Applications*, Cambridge University Press.

[39] Malhotra, P. K. (2000). "Practical Nonlinear Seismic Analysis of Tanks," *Earthquake Spectra*, Vol. 16, No. 2, pp. 473-492.

[40] Vathi, M., Pappa, P., and Karamanos, S. A. (2013). "Seismic Response of Unanchored Liquid Storage Tanks," *ASME 2013 Pressure Vessels & Piping Division Conference,* PVP2013-97700, Paris, France.

[41] Vathi, M., and Karamanos, S. A. (2014). "Modeling of Uplifting Mechanism in Unanchored Liquid Storage Tanks Subjected to Seismic Loading," *2nd European Conference on Earthquake Engineering and Seismology* (2ECEES), 24-29 August 2014, Istanbul, Turkey.

[42] Malhotra, P. K., and Veletsos, A. S. (1994). "Uplifting Response of Unanchored Liquid-Storage Tanks", *Journal of Structural Engineering*, Vol. 120, No. 12, pp. 3525-3547.

[43] Prinz, G. S., and Nussbaumer, A. (2012). "Fatigue analysis of liquid-storage tank shell-to-base connections under multi-axial loading," *Engineering Structures*, Vol. 40, pp. 77-82.

[44] Vathi, M., and Karamanos, S. A. (2015). "Simplified Model for the Seismic Response of Unanchored Liquid Storage Tanks," *ASME 2015 Pressure Vessels & Piping Division Conference,* PVP2015-45695, Boston, Massachusetts, USA.

[45] American Petroleum Institute (2013). *Welding of Pipelines and Related Facilities.* API Standard 1104, 21st Edition, Washington, DC.

[46] European Committee for Standardization (2006). *Design of Joints, Eurocode 3, Part 1-8*, CEN/TC 250, EN 1993-1-8, Brussels.

[47] Pappa, P., Vasilikis, D., Vazouras, P., and Karamanos, S. A. (2011). "On the Seismic Behaviour and Design of Liquid Storage Tanks." *III ECCOMAS Thematic Conference on Computational Methods in Structural Dynamics and Earthquake Engineering.* COMPDYN 2011, Corfu, Greece.

[48] Natsiavas, S., Babcock, C. D. (1987). "Buckling at the top of a fluid-filled tank during base excitation.", *Journal of Pressure Vessel Technology*, ASME, Vol. 109, No. 4, pp. 374-380.

[49] De Angelis, M., Giannini, R., Paolacci, F. (2010). "Experimental investigation on the seismic response of a steel liquid storage tank equipped with floating roof by shaking table tests", *Earthquake Engineering and Structural Dynamics*, Vol. 39, No. 4, pp. 377-396.

[50] HAZUS (1997). "Earthquake Loss Estimation Methodology," *National Institute of Building Sciences*, prepared by Risk Management Solutions, Menlo Park, CA, USA.

[51] American Lifelines Alliance (2001). *Seismic Fragility Formulations for Water Systems,* Part-1 – Guidelines, Report.

[52] Karamanos, S. A., Giakoumatos, E. and Gresnigt, A. M. (2003). "Nonlinear Response and Failure of Steel Elbows Under In-Plane Bending and Pressure.", *Journal of Pressure Vessel Technology*, ASME, Vol. 125, No. 4, pp. 393-402.

[53] Okeil, A. M., Tung, C. C. (1996). "Effects of ductility on seismic response of piping systems and their implication on design and qualification", *Nuclear Engineering and Design*, Vol. 166, No. 1, pp. 69-83.

[54] Canadian Standard Association (2007). *Oil and Gas Pipeline Systems*, CSA-Z662, Mississauga, Ontario, Canada.

[55] Gresnigt, A. M. (1986). "Plastic Design of Buried Steel Pipelines in Settlement Areas", *Heron*, Vol. 31. No. 4, Delft, The Netherlands.

[56] Veletsos, A. S., and Tang, Y. (1987). "Rocking Response of Liquid Storage Tanks," *Journal of Engineering Mechanics*, Vol. 113, No. 11, pp. 1774-1792.

[57] Veletsos, A. S., and Yang, J. Y. (1977). "Earthquake Response of Liquid Storage Tanks," *2nd ASCE Engineering Mechanics Conference*, Raleigh, NC, pp. 1-24.

[58] Vathi, M., and Karamanos, S. A. (2014). "Liquid Storage Tanks: Seismic Analysis," *Encyclopedia of Earthquake Engineering*, Article: 368990, Chapter: 144, Springer.

[59] De Grassi, G., Nie, J., and Hofmayer, C. (2008). *Seismic Analysis of Large-Scale Piping Systems for the JNES-NUPEC Ultimate Strength Piping Test Program*, NUREG/CR-6983, Brookhaven National Laboratory, Upton, NY.

[60] Karamanos, S. A. (2016). "Mechanical Behavior of Steel Pipe Bends; An Overview.", *Journal of Pressure Vessel Technology*, ASME, Invited paper: special issue for the 50th Anniversary of PVPD, in press.

[61] Karamanos, S. A. and Tassoulas, J. L. (1996a). "Tubular Members I: Stability Analysis and Preliminary Results.", *Journal of Engineering Mechanics*, ASCE, Vol. 122, No. 1, pp.64-71.

[62] Simulia (2012). ABAQUS *User's Manual*, Version 6.12.

[63] van der Vegte, G. J., de Back, J., Wardenier, J., (1989). "Low Cycle Fatigue of Welded Structures", Stevin Report, 25.6.89.09/A1.

[64] British Standards Institution (1993). *Fatigue Design and Assessment of Steel Structures*, BS 7608 standard, UK.